On modified Keplerian dynamics (MoKD)

Brent Jarvis
Embry−Riddle Aeronautical University
MoKDContact@gmail.com

Abstract:

Orbits are parameterized with the space−time dimensions of the gravitational constant ($\mathbb{R}^3$, t^2). Novel solutions for the flyby anomaly, dark matter, and the gravitational lensing effect are deduced from first principles. Observable evidence is provided with several experimental predictions to test the modified Keplerian dynamics (MoKD) hypothesis.

Introduction

It will be shown that the kinematics of a secondary's orbit can be parameterized with the space−time dimensions of the gravitational constant $(\mathbb{R}^3, \mathbf{t}^2)$:

$$\textbf{[1a]}\quad \begin{bmatrix} x(t_1,t_2) \\ y(t_1,t_2) \\ z(t_1,t_2) \end{bmatrix} = \begin{bmatrix} (r_1 + r_2\cos(t_2))\cos(t_1) \\ (r_1 + r_2\cos(t_2))\sin(t_1) \\ r_2\sin(t_2) \end{bmatrix};\ \begin{bmatrix} t_1 \\ t_2 \end{bmatrix} \in \begin{bmatrix} 0, \dfrac{(\pm)\bullet_1|T_{S1}|}{|T_1|} \\ 0, \dfrac{(\pm)\bullet_2|T_{S1}|}{|T_2|} \end{bmatrix} \rightarrow \begin{bmatrix} 0, \dfrac{(\pm)\bullet_1|T_{S2}|}{|T_1|} \\ 0, \dfrac{(\pm)\bullet_2|T_{S2}|}{|T_2|} \end{bmatrix} \cdots \begin{bmatrix} 0, \dfrac{(\pm)\bullet_1|T_{Sn}|}{|T_1|} \\ 0, \dfrac{(\pm)\bullet_2|T_{Sn}|}{|T_2|} \end{bmatrix};$$

(Orbit is exaggerated for clarity)

[1b]

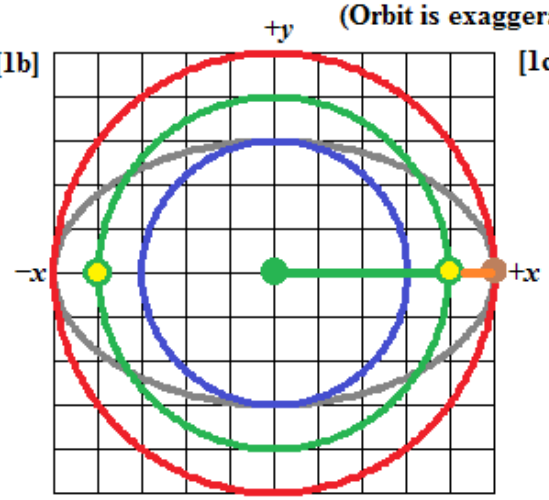

[1c]

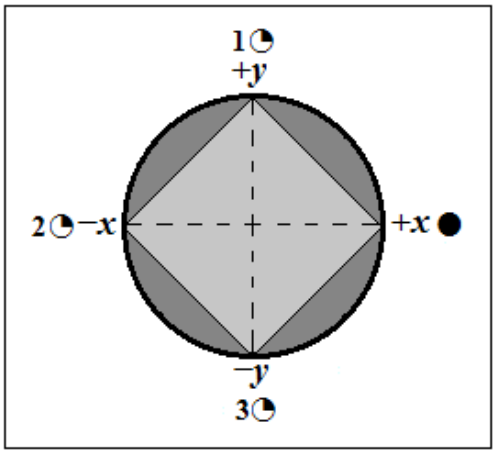

Focus Centroid Secondary Keplerian Ellipse r_1 r_2 $[-x, +x]$ Line of Apsides

Circumference of r_A Circumference of r_1 Circumference of r_B

$$\textbf{[1d]}\quad ◔ = \frac{○}{□} = \frac{\pi}{2};\ ● = 4◔;\ r_A = \frac{r_{E(+)} + r_{E(-)}}{2};\ r_B = \frac{r_{T(+)} + r_{T(-)}}{2};\ r_1 = \frac{r_A + r_B}{2};\ r_2 = r_A - r_1;$$

$$|T_S| = \frac{\bullet_1 r_1}{v_T};\ |T_1| = \frac{\bullet_1 r_A}{v_T};\ |T_2| = \frac{\bullet_2 r_2}{v_P};$$

The parametric equation **[1a]** will be referred to as a halo. The halo assumes an isolated 2−body system (*n*−bodies will be discussed in a subsequent paper). A 2−D graph of a halo is shown in **[1b]** (the foci of the ellipse are overlapped due to the exaggerated eccentricity of the orbit and the line of apsides is inclined relative to the equatorial plane of the primary body.) The definitions of the halo space−time parameters are given in **[1d]**, where ◔ is the ratio between the areas of a unit circle (○) and a square (□) formed by the hypotenuses of the [***x***, ***y***] plane of the circle as seen in **[1c]**. The symbol ● = 4◔ = **2π**, and ● will be referred to as a clock. The radius of a positive clock sweeps out sectors in a counterclockwise direction while the radius of a negative clock sweeps out sectors in a clockwise direction. A (−) sign does not indicate a reversal in time. Analogous to a linearly polarized electromagnetic field, the [$\mathbf{t_1}$, $\mathbf{t_2}$] clocks are orthogonal to each other. The radius of the $\mathbf{t_2}$ clock ($\bullet_2$) alternates its direction relative to an inertial frame of reference due to the mirror symmetry of a halo (i.e the radius of $\bullet_2$ is a pseudovector):

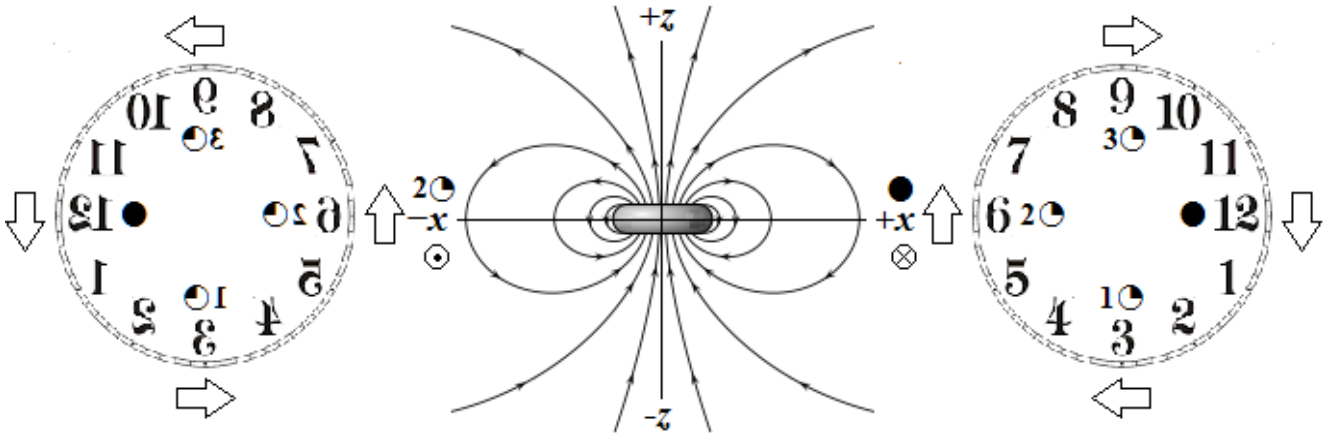

I refer to this as the transparent clock effect; if you spin a transparent clock over by **2◔ = 6:00 = 180º** it appears as if the clock is ticking counterclockwise relative to your frame of reference but it continues to tick clockwise. The $\mathbf{t_2}$ clock in the above image is over exaggerated; the compactified temporal dimension $\mathbf{t_2}$ is miniscule relative to $\mathbf{t_1}$ for planetary orbits since $\bullet_1\mathbf{r_1} >> \bullet_2\mathbf{r_2}$. The temporal dimension $\mathbf{t_1}$ is taken at periapsis while $\mathbf{t_2}$ is taken at the secondary's ascending node ($\mathbf{t_1}$ and $\mathbf{t_2}$ are phase shifted as we will see in the next section). Further information regarding compactified temporal dimensions can be found in thermal quantum field theory.[1, 2, 3]

For an elliptical orbit, the variables $\mathbf{r_A}$ and $\mathbf{r_B}$ are the secondary's mean eccentric anomaly distance (the semi-major axis of the ellipse) and mean true anomaly distance (the semi-minor axis) respectively, $\mathbf{r_1}$ is the mean distance between $\mathbf{r_A}$ and $\mathbf{r_B}$, and $\mathbf{r_2}$ is the difference between $\mathbf{r_A}$ and $\mathbf{r_1}$. The variables $|\mathbf{T_1}|$ and $|\mathbf{T_2}|$ are the orthogonal toroidal and poloidal periods (anomalistic and tropical respectively) and $|\mathbf{T_S}|$ is the secondary's sidereal period. Apsidal precession is modeled with a halo due to the circumferential difference between $\bullet\mathbf{r_A}$ and $\bullet\mathbf{r_1}$ relative to the secondary's toroidal mean motion $\mathbf{v_T}$. The quantities $\bullet\mathbf{r_1}$ and $\bullet\mathbf{r_2}$ are the circumferences of the halo's toroidal and poloidal axes respectively, and $\mathbf{v_P}$ is the secondary's poloidal mean motion ($\mathbf{v_T} >> \mathbf{v_P}$ for the planets in our solar system.) Keeping with convention, the temporal dimensions are measured in sidereal years and the spatial dimensions are measured in astronomical units **AU** (the length of $\mathbf{r_1}$, however, is slightly less than **1 AU** for the earth's orbit ≈ **0.9998252 AU** and the length of $\mathbf{r_2} \approx \mathbf{0.0001748\ AU} \approx \mathbf{2.05}\varnothing_E$ in the J2000.0 epoch, where $\varnothing_E$ is the earth's diameter.) The secondary's position can be graphed with the vector value function:

$$[2]\ \vec{\mathbf{r}}(t_1, t_2) = (r_1 + r_2 \cos(t_2)) \cos(t_1)\,\hat{i} + (r_1 + r_2 \cos(t_2)) \sin(t_1)\,\hat{j} + r_2 \sin(t_2)\hat{k}.$$

A secondary's halo orbit can be intuitively modeled as an inertial point upon the surface area of an infinitesimally viscous smoke ring (a toroidal Higgs condensate.) A smoke ring is naturally 5−D since two temporal dimensions are required in order to parameterize its motion relative to its toroidal and poloidal degrees of freedom (i.e abstract dimensions are not required in order to model the secondary's motion). A similar framework was discovered independently by Ken Barker from observing the kinematics of gas and dust in the Centaurus A galaxy. In Barker's Harvard publication entitled "*Nested elliptical orbits and their resemblance to a rolling torus structure*"[4] he gave the following equivalencies for ellipses and tori:

set of ellipses	paths within the torus
$R_{max} = a(1+e)$	$R_{max} = R(1+r/R)$
$R_{min} = (1-e)$	$R_{min} = R(1-r/R)$
semi major axis a is equivalent to R and eccentricity e is equivalent to r/R	
eccentricity $= e$	pseudo-eccentricity $e' = r/R$
semi-minor axis $= a\sqrt{(1-e^2)}$	semi "minor axis" $= R\sqrt{(1+e'^2)}$
$\sin i = e$	$\tan i = r/R = e'$
max. torus thickness $= 2ae\sqrt{(1-e^2)}$	max. torus thickness $= 2Re' = 2r$
max. thickness is at radius $= a(1-e^2)$	max. thickness is at radius $= R$

The primary difference between Barker's findings and the halo model (excluding the extra temporal dimension) is that the Keplerian semi-major axis **a** and semi-minor axis **b** are equivalent to $\mathbf{a} = \mathbf{r_A}$ and $\mathbf{b} = \mathbf{r_B}$. The radii $\mathbf{r_1}$ and $\mathbf{r_2}$ form the toroidal and poloidal axes of rotation for a halo.

Observable evidence

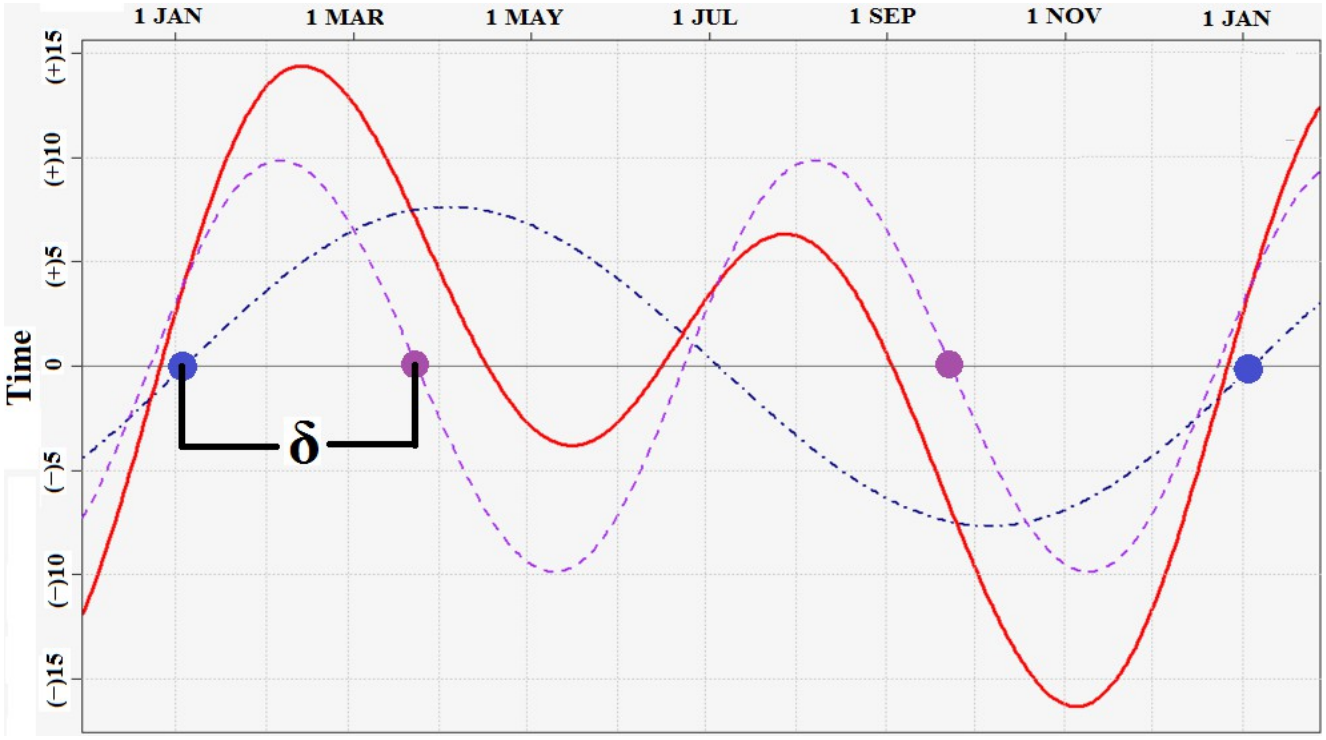

FIG. 1: An equation of time graph.

The red curve in the equation of time graph above represents the cumulative time discrepancy between apparent and mean solar time on earth (the (+) sign indicates an accurate watch ticking faster than time read from a sundial and the (−) sign indicates the opposite). The blue dash & dot toroidal temporal wave has a nodal period (marked with the blue dots) which is slightly greater than a sidereal year and an amplitude of ≈ **7.66** minutes. The mauve dashed poloidal (obliquity) temporal wave has a nodal period of approximately half a sidereal year (marked with the mauve dots) and an amplitude of ≈ **9.87** minutes. Due to the phase shift **δ ≈** ◔ between the temporal waves (precession), the earth's poloidal period $|\mathbf{T_2}|$ is taken at its ascending node (vernal equinox) while $|\mathbf{T_1}|$ is taken at perihelion, each period being relative to the earth's sidereal period $|\mathbf{T_S}|$ (determined from the Barycentric celestial reference system (BCRS) created in 2000 by the International Astronomical Union.)

If the earth's temporal waves are separated into two channels on an oscilloscope in the X−Y mode the result resembles a Lissajous curve:

$$[3]\quad \begin{bmatrix} x_{CH1}(T_1) \\ y_{CH2}(T_2) \end{bmatrix} = \begin{bmatrix} A\cos(T_1 - \delta_x) \\ B\cos(T_2 - \delta_y) \end{bmatrix};$$

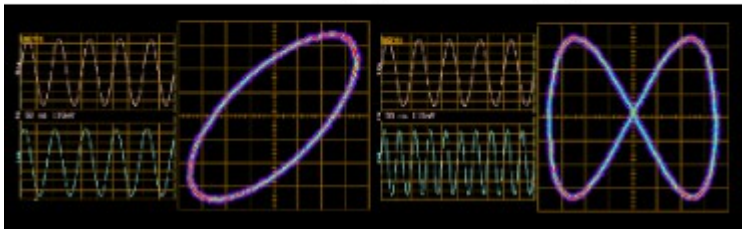

(the oscilloscope diagrams are not to scale with **FIG. 1**) where **A** and **B** are the amplitudes of $\mathbf{T_1}$ and $\mathbf{T_2}$ respectively relative to the equatorial plane of the primary body. The oscilloscope reading on the right is produced when $\mathbf{T_1{:}T_2 = 2{:}1}$, which is observed in the earth's solar analemma ($\mathbf{T_1{:}T_2 \approx 2{:}1}$ due to the phase shift $\boldsymbol{\delta} \approx$ ◔ and the [x, y] planes are rotated by ◔):

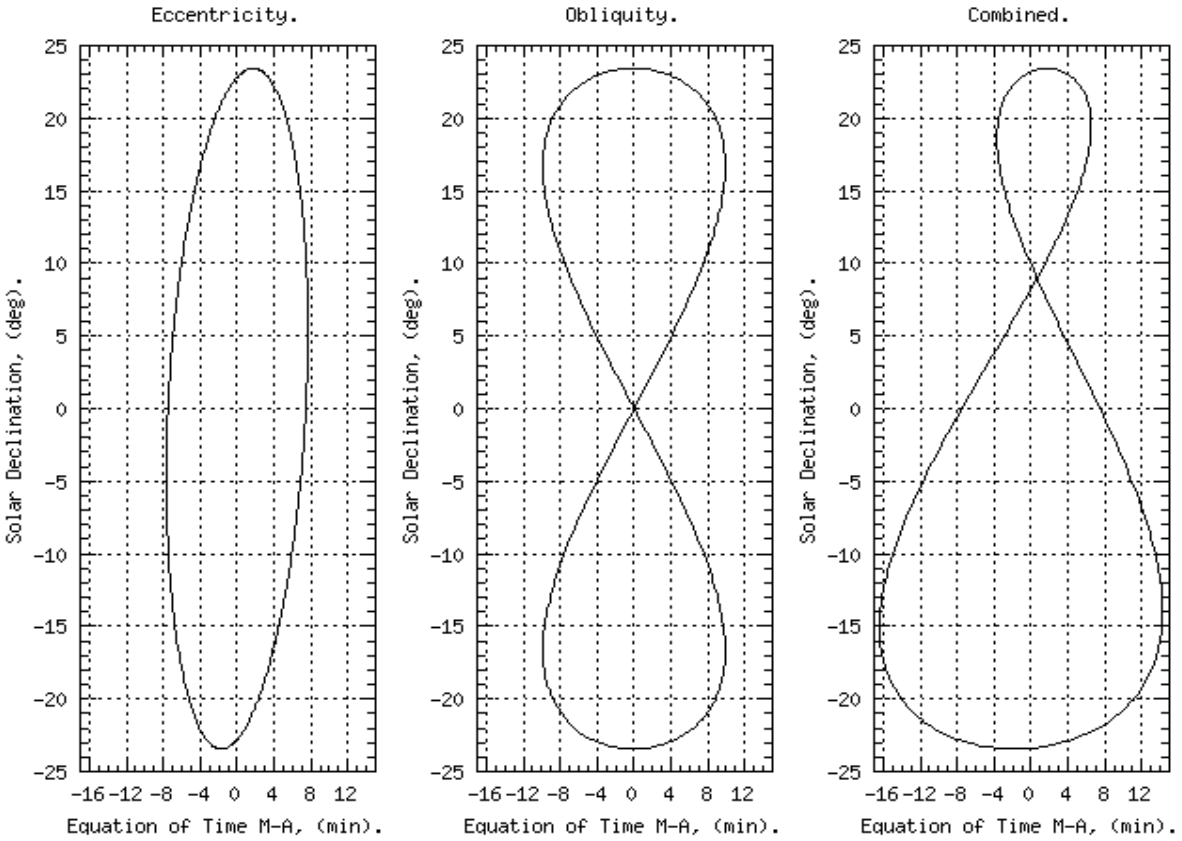

The oscilloscope reading to the left in equation [**3**] results when $\mathbf{T_1{:}T_2 = 1{:}1}$, which is observed in the

solar analemmas of Mars, Jupiter, and Saturn ($\mathbf{T_1{:}T_2 \approx 1{:}1}$):

Dark matter & gravitational lensing

Variations in a star's distance from the nucleus of a galaxy is difficult to determine with high precision. We do know, however, that the mass interior to our solar system's orbit can be estimated by assuming a circular orbit with the formula:

$$[4]\ m_1 \approx \frac{rv^2}{G}$$

where $\mathbf{m_1}$ is the estimated interior mass, **r** and **v** are our system's estimated radius and velocity respectively, and **G** is the gravitational constant. When Kepler and Newton developed their laws nearly 350 years ago it was not possible for them to observe the motion of stars as they orbit a galaxy. Their laws are based upon the assumption that all celestial orbits are limited to conic sections, but modern geological evidence[5] indicates this may not be accurate. According to the evidence, our sun oscillates relative to the galactic plane in ≈ **33 ± 1 Myr** cycles during its estimated **225−250 Myr** revolution. The sinusoidal periodicity of the sun's orbit cannot be modeled strictly with conic sections. An elliptical conic section, however, can be shown to be sinusoidal relative to a planar frame of reference:

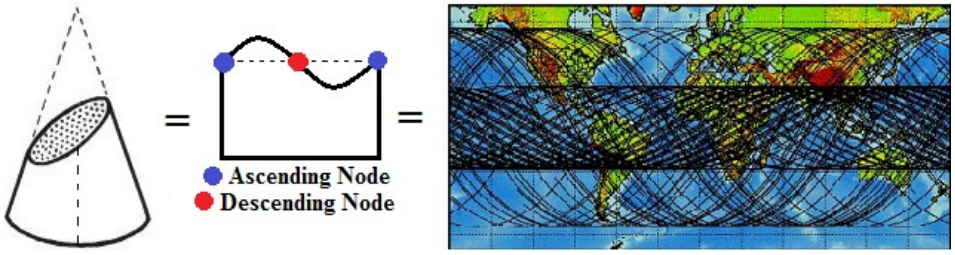

FIG 2: An elliptical conic section cut and flattened upon a 2−D surface geometrically produces a periodic wave.

Since the evidence[5] suggests a solar system's orbit may be sinusoidal, a quantized wavenumber parameter for galactic systems will be assumed:

$$[5]\ N_T = \frac{n_T - 1}{2}$$

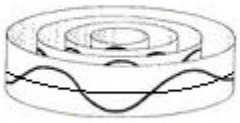

$$N_T = 1, 2, 3, 4 \ldots n$$

where $\mathbf{N_T}$ is the system's toroidal wavenumber and $\boldsymbol{n_T}$ is its total number of ascending and descending

nodes relative to the galactic plane (the initial node is subtracted since the system's orbit is recursive.) Using the geological evidence[5] we can then approximate our sun's toroidal wavenumber. The rounded average between **225** and **250** is **238**, and **238 / 34 = 7** (assuming an integer value.) From equation **[5]** we obtain $\mathbf{N_T \approx (7-1) / 2 \approx 3}$. Combining equation [**4**] with [**5**], the estimated mass within our solar system's radius is hypothesized to be:

$$[6] \sum_{i=m_{01}}^{m_{0n}} m_0 \approx \left(\frac{r_1 v_T^2}{N_T G}\right) - m_{0S}$$

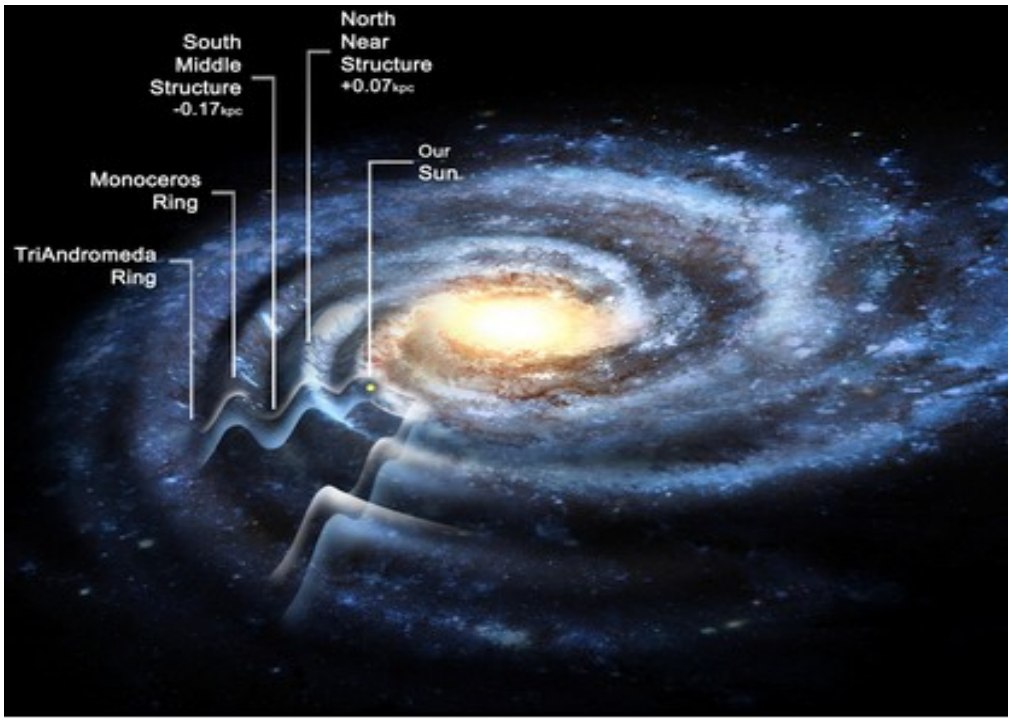

FIG. 3: The observed wave characteristics of our Milky Way galaxy.

where $\mathbf{m_0}$ is the rest mass of the bodies interior to our system's orbit and $\mathbf{m_{0S}}$ is the sun's rest mass. Since **m** and **G** are constants (excluding special relativistic effects) a system's toroidal wave quantity increases as the radius of its halo orbit increases and vice versa. The consistency in a star's orbital speed, independent upon its radial distance from the galactic nucleus, is hypothetically due to the conservation of the secondary's poloidal angular momentum. This can be tested experimentally by observing the aggregated poloidal arc of a system's halo orbit. Systems with a distance from the nucleus ≤ the sun's distance should be observed to have $\mathbf{N_T \leq 3}$ and systems with a distance > the sun's distance should be observed to have $\mathbf{N_T > 3}$ (being dependent upon their rest mass). It is recommended that systems with a relatively greater radius be studied initially since their poloidal mean motion is greater according to the halo hypothesis, preferably in the region spanning from the North Near Structure and TriAndromeda Ring illustrated in **FIG. 3** above.

What about the gravitational lensing effect? We know from Newton's laws of motion that a secondary does not orbit a primary, both bodies orbit a common center of mass point. From Kepler and Newton's temporal equation:

$$[7] \; T_S = \bullet \sqrt{\frac{r_A^3}{G m_1}},$$

it is hypothesized that the "virtual mass point" $\mathbf{m_V}$ of a secondary's poloidal orbit is:

$$[8]\ \sqrt{m_V} = \frac{(\pm)\bullet_2}{|T_2|}\sqrt{\frac{r_2^3}{G}},$$

A relatively recent (2008) paper published by Stephen Adler[6] suggests the flyby anomaly can be attributed to dark matter in the earth's vicinity and several other papers[7, 8, 9] listed in the references support this hypothesis. According to the halo model, the approximate distance of the earth's virtual mass point is ≈ **2.05ø**$_E$ from its center, and it would have a polar orbit relative to the earth's position instead of the conventional equatorial orbit. Possible video evidence for the earth's virtual mass point transiting the moon can be found in the references,[10] although it is NOT a credible source and the author unwittingly assumes it is a U.F.O. Further investigation is required in order to rule out the likely possibility that the transiting dark spot is a satellite, but a similar transit can be predicted with the halo hypothesis.

Fundamentally, the missing "matter" in a galaxy is missing "mass", but it is assumed that the missing mass must be materialistic. It is well known that there are certain points in space-time, such as Lagrangian points, which influence the motion of celestial bodies. It is hypothesized that the virtual mass points in the intergalactic arena have the required Higgs field density to influence the motion of matter and energy. Images of the gravitational lensing effect suggest this may be true since dark "matter" is confined to certain point−like regions of space-time and not widely distributed:

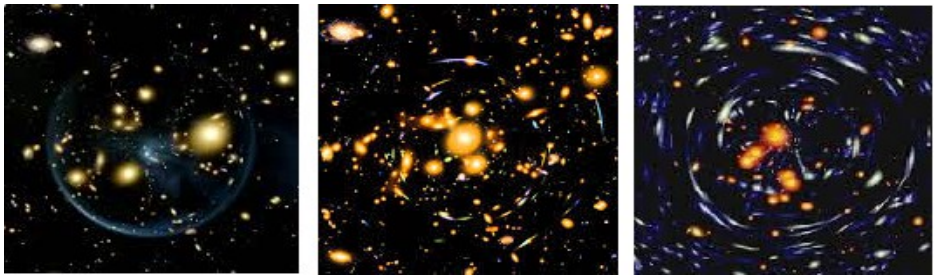

There is another interesting gravitational lensing effect that can be deduced from the halo model. Due to the space-time geometry of a halo, a galaxy's luminosity may appear to be blueshifted despite the observed expansion of space:

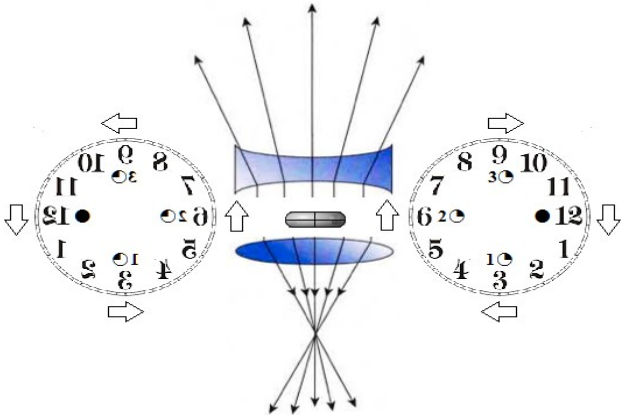

FIG. 4: A pictorial analogy of light rays passing through a concave and convex lens relative to the *z*−axis of a halo. As space-time diverges from 2◔ to ● the light rays diverge as if they have passed through a concave lens. As space−time converges from ● to 2◔ the light rays converge towards a focal point as if they have passed through a convex lens.

Several unexplained blueshifted galaxies are observed in the direction of the Virgo cluster,[11, 12, 13] such as M90, M86, M98, IC 3258, NGC 4419, and RMB 56, indicated by the blue arrows in the MEGASTAR diagram below:

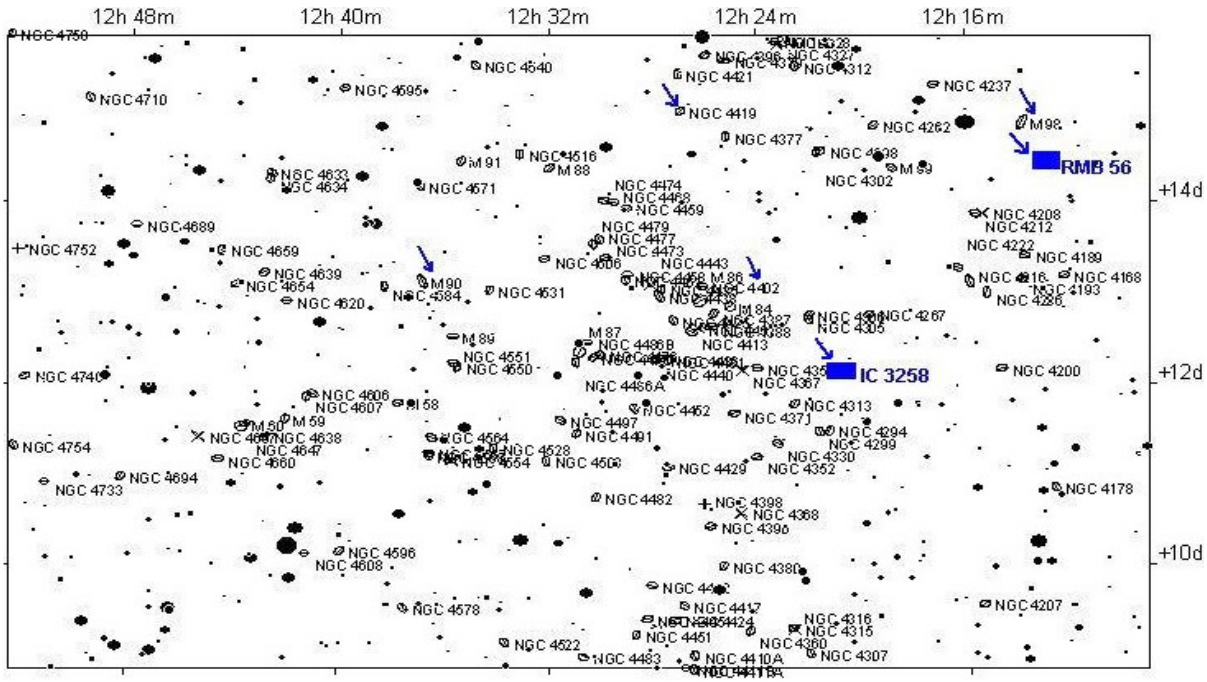

FIG. 5: Galaxies in the region of the Virgo Cluster seem to contradict the spatial expansion model.

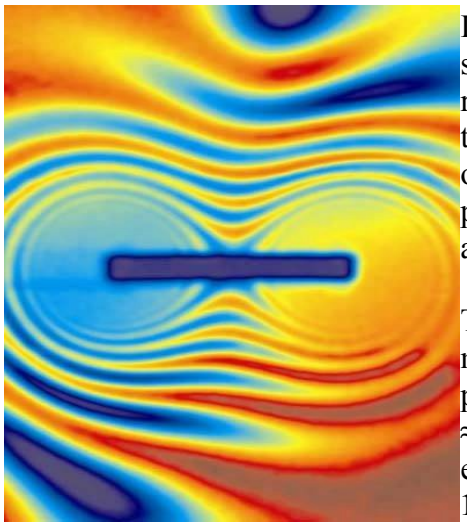

It is hypothesized that each of the anomalous blueshifted galaxies share a common rotational direction relative to our frame of reference, and what we perceive as a blueshift is the contraction of the galaxy's wavelengths. It should also be considered that the observed accelerated expansion of space may be due to our relative position within the Milky Way. For instance, we may be located in a “red zone” region where the geometry of space-time is divergent.

There are several other predictions that can be made with the halo model, such as spin−orbit coupling, an aphelion precession > perihelion precession for Venus, longitudinal gravity waves, a $\mathbf{T_1:T_2 \approx 2:1}$ Polaris analemma, virtual mass gravity assists, and a minute elongation of the semi-minor axis of the planets that have $\mathbf{T_1:T_2 \approx 1:1}$, all of which will be subjects of a subsequent paper.

Conclusion

The space-time dimensions of the gravitational constant were used as first principles to deduce the origin of dark “matter” and the gravitational lensing effect. Several intriguing predictions can be made with the halo model and it is supported by observable evidence. If stellar systems have wave characteristics as they orbit galactic nuclei, the kinematics of the macrocosm may be homogenous to the kinematics of quantum systems. Also, by mapping out the relative positions of virtual mass points, it may be possible in the future to more efficiently travel through space-time.

Dedication

This paper is dedicated to Cynthia Cashman Lett, without whom it would not have been published.

References

[1] Zinn-Justin, Jean (2000). "*Quantum field theory at finite temperature: An introduction*". arXiv:hep-ph/0005272 [hep-ph].

[2] N.P. Landsman and Ch.G. van Weert (1987). "*Real- and imaginary-time field theory at finite temperature and density*". *Physics Reports* 145 (3-4): 141–249.

[3] T.S. Evans and D.A. Steer (1996). "*Wick's theorem at finite temperature*". *Nucl.Phys.B* 474 (2): 481–496. arXiv:hep-ph/9601268.

[4] K. Barker (1999). "*Nested elliptical orbits and their resemblance to a rolling torus structure*". Monthly Notices of the Royal Astronomical Society, Volume 306, Issue 2, pp. 509-512.

[5] M.R. Rampino and R.B. Stothers (1984). "*Terrestrial mass extinctions, cometary impacts, and the Sun's motion perpendicular to the galactic plane*," Nature 308, 709 – 712.

[6] S.L. Adler (2008). "*Can the flyby anomaly be attributed to earth−bound dark matter?*" arXiv:0805.2895

[7] C. Lammerzahl, O. Preuss, and H. Dittus (2006). "*Is the physics within the Solar system really understood?*" arXiv:gr-qc/ 0604052.

[8] S.L. Adler (2008). "*Placing direct limits on the mass of earth-bound dark matter*", arXiv:0808.0899.

[9] X. Xu and E.R. Siegel (2008) "*Dark Matter in the Solar System*", arXiv:0806.3767.

[10] NOT CREDIBLE: **https://www.youtube.com/watch?v=KyT0qwJ9uHo**

[11] E.M Burbidge and M.H Demoulin (1969). "*IC 3258, A Small Extragalactic Object with a Blueshift",* Astrophysical Journal, 157, L155.

[12] T.D. Kinman (1977). "*Compact Blueshifted Galaxy RMB 56 (1216+141)*", Astronomical Journal, 82, p. 879.

[13] G.A. Tammann (1972). "*Remarks on the Radial Velocities of Galaxies in the Virgo Cluster*", Astronomy & Astrophysics, 21, p. 355.